Physics Letters B 806 (2020) 135474

Contents lists available at ScienceDirect

Physics Letters B

www.elsevier.com/locate/physletb

Pairing-quadrupole interplay in the neutron-deficient tin nuclei: First lifetime measurements of low-lying states in ^{106,108}Sn

M. Siciliano [a,b,c,*], J.J. Valiente-Dobón [a], A. Goasduff [a,b,d], F. Nowacki [e], A.P. Zuker [e], D. Bazzacco [d], A. Lopez-Martens [f], E. Clément [g], G. Benzoni [h], T. Braunroth [i], F.C.L. Crespi [h,j], N. Cieplicka-Oryńczak [h,1], M. Doncel [k], S. Ertürk [l], G. de France [g], C. Fransen [i], A. Gadea [m], G. Georgiev [f], A. Goldkuhle [i], U. Jakobsson [n], G. Jaworski [a,2], P.R. John [b,d,3], I. Kuti [o], A. Lemasson [g], T. Marchi [a], D. Mengoni [b,d], C. Michelagnoli [g,4], T. Mijatović [r], C. Müller-Gatermann [i], D.R. Napoli [a], J. Nyberg [p], M. Palacz [q], R.M. Pérez-Vidal [m], B. Sayğı [a,5], D. Sohler [o], S. Szilner [r], D. Testov [b,d], M. Zielińska [c], D. Barrientos [s], B. Birkenbach [i], H.C. Boston [t], A.J. Boston [t], B. Cederwall [n], J. Collado [u], D.M. Cullen [v], P. Désesquelles [f], C. Domingo-Pardo [m], J. Dudouet [f,6], J. Eberth [i], F.J. Egea-Canet [a], V. González [u], L.J. Harkness-Brennan [t], H. Hess [i], D.S. Judson [t], A. Jungclaus [w], W. Korten [c], M. Labiche [x], A. Lefevre [g], S. Leoni [h,j], H. Li [n], A. Maj [y], R. Menegazzo [d], B. Million [h], A. Pullia [h,j], F. Recchia [b,d], P. Reiter [i], M.D. Salsac [c], E. Sanchis [u], O. Stezowski [z], Ch. Theisen [c]

[a] INFN, Laboratori Nazionali di Legnaro, Legnaro (PD), Italy
[b] Dipartimento di Fisica e Astronomia, Università di Padova, Padua (PD), Italy
[c] CEA/Irfu/DPhN, Université de Paris-Saclay, Gif-sur-Yvette, France
[d] INFN, Sezione di Padova, Padua, Italy
[e] IPHC, CNRS/IN2P3 Université de Strasbourg, Strasbourg, France
[f] CSNSM, CNRS/IN2P3, Université de Paris-Saclay, Orsay, France
[g] Grand Accélérateur National d'Ions Lourds, CEA/Irfu/DRF and CNRS/IN2P3, Caen, France
[h] INFN, Sezione di Milano, Milan, Italy
[i] Institut für Kernphysik, Universität zu Köln, Cologne, Germany
[j] Dipartimento di Fisica, Università di Milano, Milan, Italy
[k] Universidad de Salamanca, Salamanca, Spain
[l] Ömer Halisdemir Üniversitesi, Niğde, Turkey
[m] Instituto de Física Corpuscular, CSIC-Universidad de Valencia, Valencia, Spain
[n] Department of Physics, Royal Institute of Technology, Stockholm, Sweden
[o] INR, Hungarian Academy of Sciences, Debrecen, Hungary
[p] Department of Physics and Astronomy, Uppsala University, Uppsala, Sweden
[q] Środowiskowe Laboratorium Ciężkich Jonów, Uniwersytet Warszawski, Warsaw, Poland
[r] Ruđer Bošković Institute and University of Zagreb, Zagreb, Croatia
[s] CERN, Geneva, Switzerland
[t] Oliver Lodge Laboratory, University of Liverpool, Liverpool, UK
[u] Departamento de Ingeniería Electrónica, Universitad de Valencia, Valencia, Spain
[v] Schuster Laboratory, University of Manchester, Manchester, UK
[w] Instituto de Estructura de la Materia, CSIC, Madrid, Spain
[x] STFC Daresbury Laboratory, Warrington, UK
[y] Instytut Fizyki Jądrowej im. Henryka Niewodniczańskiego, Polska Akademia Nauk, Krakow, Poland
[z] IPN-Lyon, CNRS/IN2P3, Université de Lyon, Villeurbanne, France

* Corresponding author at: CEA/Irfu/DPhN, Université de Paris-Saclay, Gif-sur-Yvette, France.
E-mail address: marco.siciliano@lnl.infn.it (M. Siciliano).
[1] Present address: *Instytut Fizyki Jądrowej im. Henryka Niewodniczańskiego, Polska Akademia Nauk, Krakow, Poland.*
[2] Present address: *Środowiskowe Laboratorium Ciężkich Jonów, Uniwersytet Warszawski, Warsaw, Poland.*
[3] Present address: *Institut für Kernphysik, Technische Universität Darmstadt, Darmstadt, Germany.*
[4] Present address: *Institut Laue-Langevin, Grenoble, France.*
[5] Present address: *Ege Üniversitesi, İzmir, Turkey.*
[6] Present address: *IPN-Lyon, CNRS/IN2P3, Université de Lyon, Villeurbanne, France.*

https://doi.org/10.1016/j.physletb.2020.135474

ARTICLE INFO

Article history:
Received 24 December 2019
Received in revised form 27 March 2020
Accepted 4 May 2020
Available online 11 May 2020
Editor: B. Blank

Keywords:
Lifetime
Nuclear structure
Multi-nucleon transfer
Light Sn
Tracking array

ABSTRACT

The lifetimes of the low-lying excited states 2^+ and 4^+ have been directly measured in the neutron-deficient ^{106,108}Sn isotopes. The nuclei were populated via a deep-inelastic reaction and the lifetime measurement was performed employing a differential plunger device. The emitted γ rays were detected by the AGATA array, while the reaction products were uniquely identified by the VAMOS++ magnetic spectrometer. Large-Scale Shell-Model calculations with realistic forces indicate that, independently of the pairing content of the interaction, the quadrupole force is dominant in the $B(E2; 2_1^+ \rightarrow 0_{g.s.}^+)$ values and it describes well the experimental pattern for $^{104-114}$Sn; the $B(E2; 4_1^+ \rightarrow 2_1^+)$ values, measured here for the first time, depend critically on a delicate pairing-quadrupole balance, disclosed by the very precise results in ^{108}Sn.

1. Introduction

A little over a decade ago, the Sn isotopes were considered the paradigms of pairing dominance: low-lying states of good seniority, nearly constant $J^\pi = 2_1^+$ excitation energies and parabolic $B(E2; 2_1^+ \rightarrow 0_{g.s.}^+)$ behavior. The latter was observed for $A \geq 116$. For the lighter species, experimental results on transition probabilities were scarce as the presence of low-lying isomeric states hindered direct measurements of lifetimes below them. From Coulomb-excitation measurements with radioactive ion beams only the reduced transition probability between the first excited 2^+ state and the ground state could be determined [1–8]. Within experimental uncertainties, they suggest a rather-constant behavior for $106 \leq A \leq 110$, instead of the parabolic trend expected when isovector $T = 1$ pairing dominates. This "plateau" includes also the stable ^{112,114}Sn nuclei, for which measurements of both $B(E2; 2_1^+ \rightarrow 0_{g.s.}^+)$ and $B(E2; 4_1^+ \rightarrow 2_1^+)$ values exist [9]. Before this work, the $B(E2; 4_1^+ \rightarrow 2_1^+)$ values were completely absent in the neutron-deficient Sn isotopes.

The experiment described in this Letter was devoted to determine the strength of $2_1^+ \rightarrow 0_{g.s.}^+$ and $4_1^+ \rightarrow 2_1^+$ transitions in ^{106,108}Sn by measuring the lifetime of 2_1^+ and 4_1^+ states. Although several theoretical interpretations have been proposed [10,1,4,11,12], the evolution of the $B(E2; 2_1^+ \rightarrow 0_{g.s.}^+)$ values in the light Sn nuclei remains puzzling. The experimental and theoretical results that will be presented in this Letter provide a further insight, which reveals the underlying structure of the light tin isotopes, namely the counterbalance of quadrupole and pairing forces in the Sn isotopic chain.

2. Experiment

A multi-nucleon transfer reaction, that is commonly used to investigate neutron-rich nuclei [13–15], was unconventionally adopted to populate the Sn isotopes close to the proton drip line, so the isotopes of interest were populated in the collision of a ^{106}Cd beam and a ^{92}Mo target. The beam-target combination and beam energy were selected as a compromise between two requirements. On one hand the reaction fragments energy had to be sufficiently high to allow their identification by the spectrometer. On the other, in order to perform the lifetime measurement, the population of the states above the 6^+ isomers had to be minimized; this condition imposed an upper limit on the excitation energy and consequently on beam energy, even at the expense of the cross section to populate more exotic species. The ^{106}Cd beam, provided by the separated-sector cyclotron of the GANIL facility at an energy of 770 MeV, impinged onto a 0.8 mg/cm^2 ^{92}Mo target. The lifetime measurement was performed with the Recoil Distance Doppler-Shift (RDDS) method [16–18]. The target was mounted on the differential Cologne plunger with a 1.6 mg/cm^2 thick ^{nat}Mg degrader down stream. In order to measure the lifetimes of interest, 8 different target-degrader distances in the range 31-521 µm were used. The complete (A,Z) identification, together with the velocity vector for the projectile-like products was obtained on an event-by-event basis using the VAMOS++ spectrometer [19–21], placed at the grazing angle θ_{lab}=25°. In coincidence with the magnetic spectrometer, the γ rays were detected by the γ-ray tracking detector array AGATA [22,23], consisting of 8 triple-cluster detectors placed at backward angles in a compact configuration (18.5 cm from the target). The combination of the pulse-shape analysis [24] and the Orsay Forward-Tracking (OFT) algorithm [25] allowed to reconstruct the trajectory of the γ rays emitted by the fragments. More details about the ion identification and the analysis procedure can be found in Refs. [26,27].

3. Results

Thanks to the precise determination of the ion velocity vector and the identification of the first interaction point of each γ ray inside AGATA, Doppler correction was applied on an event-by-event basis. The magnetic spectrometer directly measured the fragments velocity after the degrader ($\beta_{after} \approx 9\%$). However, for each γ-ray transition two peaks were observed, related to its emission before and after the Mg foil: the γ rays emitted after the degrader are properly Doppler corrected, while those emitted before are shifted to lower energies because of the different velocity of the reaction fragment ($\beta_{before} \approx 10\%$). The relative intensities of the peaks as a function of the target-degrader distance are related to the lifetime of the state of interest. The areas are obtained via a χ^2-minimization fit, performed by considering a gaussian shape of the peaks, whose centroid and FWHM were constrained from the closest and longest target-degrader distance spectra, and a linear background.

The complete identification of the VAMOS++ spectrometer and the employment of a multi-nucleon transfer (MNT) mechanism allowed us to reconstruct the Total Kinetic-Energy Loss (TKEL) of the reaction. This quantity was crucial for the lifetime measurements in ^{108}Sn, since it allows us to control the direct population of the excited states [18,28], in order to reduce possible contamination from the high-lying states above the 6_1^+ isomer. For this nucleus, in fact, the energies of the $2_1^+ \rightarrow 0_{g.s.}$ (1206 keV) and $8_1^+ \rightarrow 6_1^+$ (1196 keV) transitions are similar, so traditional methods cannot be used to measure the lifetime of the 2_1^+ state: due to the position of the AGATA array and to the energy loss of the reaction fragments in the degrader, the shifted component of the $2_1^+ \rightarrow 0_{g.s.}^+$ transition coincides with the unshifted component of the $8_1^+ \rightarrow 6_1^+$ transition, as shown in Fig. 1. For this reason, a gate on the TKEL was imposed in order to reduce the population of the high-lying states

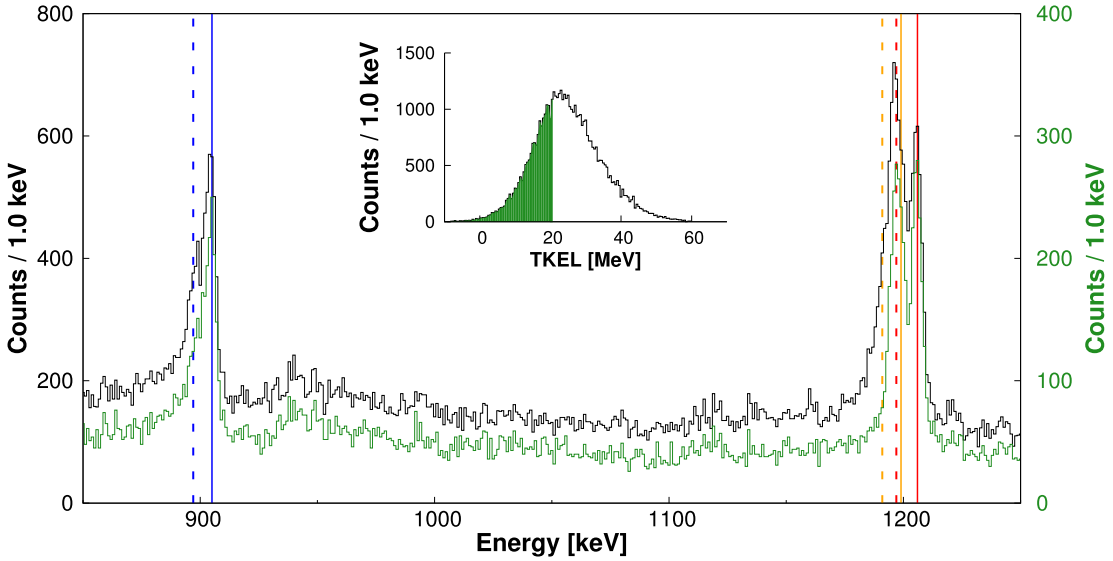

Fig. 1. Doppler-corrected γ-ray energy spectra of ^{108}Sn before (black) and after (green) the gate on the Total Kinetic-Energy Loss (TKEL), obtained by summing up the statistics of all the target-degrader distances. The $2_1^+ \rightarrow 0_{g.s.}^+$ (red), $4_1^+ \rightarrow 2_1^+$ (blue) and $8_1^+ \rightarrow 6_1^+$ (orange) transitions are marked, indicating the *unshifted* (u) and *shifted* (s) centroids with a solid and a dashed line, respectively. In the inset, the TKEL distribution and the set gate (green) are presented.

above the 6_1^+ isomer: for TKEL$<$ 21 MeV, the $8_1^+ \rightarrow 6_1^+$ transition peaks became negligible and the measured lifetime of both 4_1^+ and 2_1^+ states remained constant, even for more restrictive conditions. The determination of such a TKEL condition and its effects on the lifetime measurement are discussed in detail in Ref. [29]. In that work, the ratio of the $4_1^+ \rightarrow 2_1^+$ transition components remains constant also for larger values of the TKEL, which is consistent with the unaltered line-shape of the Fig. 1 spectra at $\approx$ 900 keV; this is due to the fact that the 6_1^+ isomer "blocks" the depopulation from higher-lying states, so their presence does not affect the lifetime measurement of the 4_1^+ state. The same is obviously true for the 2_1^+ state but, in this specific case, a blind integration of the spectrum will include the unshifted component of the $8^+ \rightarrow 6^+$ transition. Being the 8^+ a long lived state with a lifetime more than two orders of magnitude larger than the 2_1^+, this would result in an artificially shorter lifetime. For this reason, the TKEL cut allows to get rid of the contamination of our transition of interest from the 8^+ deexcitation. Fig. 2 (left) shows the Doppler-corrected γ-ray energy spectra of ^{108}Sn for several distances, requiring the TKEL$<$ 21 MeV condition. This nontraditional procedure allowed us to take into account just the 6_1^+, 4_1^+ and 2_1^+ states in the measurement of the lifetimes via Decay-Curve Method (DCM). Due to the direct population of the excited states, the presence of the long-lived 6_1^+ isomer simplifies the lifetime measurement by "blocking" the depopulation from the higher-lying states and, as shown in Fig. 2 (right), it contributes just as an offset to the decay curves of the 4_1^+ and 2_1^+ states.

For ^{106}Sn the described TKEL-gate procedure was not required and, because of the presence of the long-lived isomer, the decay cascade of the 6_1^+, 4_1^+ and 2_1^+ states was taken into account while measuring the lifetime via DCM. Also in this case, the presence of the 6_1^+ isomeric state affects the lifetime analysis by introducing an offset, which is related to the direct population of the states [17], in the decay curves of the 2_1^+ and 4_1^+ excited states. The direct population of the excited states was extracted from the single-γ spectra. This information was used to constrain the parameters of the decay curves. The possible presence of additional feeders was investigated in the single-γ spectra and also in the γ-γ coincidences: except for those considered in the measurement, no other transitions feeding the 4_1^+ and 2_1^+ excited states were observed for both ^{106,108}Sn. In Fig. 2 (right pad) the decay curves are presented

Table 1
Measured lifetime of the excited states I^π in ^{106,108}Sn and corresponding $B(E2; I^\pi \rightarrow I^\pi - 2)$ values. The last column shows the theoretical predictions from the extension of the calculations of Ref. [1] (see text).

	I^π	E_γ [keV]	τ [ps]	B(E2) [e^2 fm^4]	
				Exp.	Theo.
^{108}Sn	2_1^+	1206.1	0.76 (8)	422 (44)	425
	4_1^+	905.1	3.7 (2)	364 (20)	349
^{106}Sn	2_1^+	1207.7	1.3 (7)	245 (132)	339
	4_1^+	811.9	5 (4)	446 (334)	379

for the 4_1^+ and 2_1^+ states: the extracted lifetime of the 2_1^+ state is in perfect agreement with the literature, supporting the validity of the experimental method. Therefore, thanks to the powerful setup and the unconventional experimental technique, the lifetime of the 2_1^+ and 4_1^+ states have been measured, for the first time, in ^{106,108}Sn.

Table 1 summarizes the experimental results, showing the lifetimes and the derived reduced transition probabilities $B(E2)$ for ^{108}Sn and ^{106}Sn isotopes, as well as the theoretical values from the extension of the calculations of Ref. [1], obtained by employing the same interaction in the full *gds* valence space for both protons and neutrons, using the effective charges $(e_\pi, e_\nu) = (1.35, 0.65)$, allowing up to $4p-4h$ excitations and without any seniority truncation. The extracted $B(E2)$ values for the ^{106,108}Sn isotopes are shown in Fig. 3 together with all previous experimental results for the whole isotopic chain. The $B(E2; 2_1^+ \rightarrow 0_{g.s.}^+)$ strengths previously measured are compatible with the results obtained in this experiment, while for the $B(E2; 4_1^+ \rightarrow 2_1^+)$ values no data existed in this region. Unfortunately, the exoticity of ^{106}Sn and the necessity to avoid the population of the states above the long-lived 6^+ isomer result in a rather large statistical error on the $B(E2; 4_1^+ \rightarrow 2_1^+)$ value for this isotope.

4. Discussion

In view of the present experimental results, the interpretation of the data in the neutron-deficient tin isotopes were performed within the theoretical companion contribution by Zuker [30]. This theoretical work explores the nuclear Hamiltonian within shell-model calculations in the light Cd and Sn isotopes, considering the

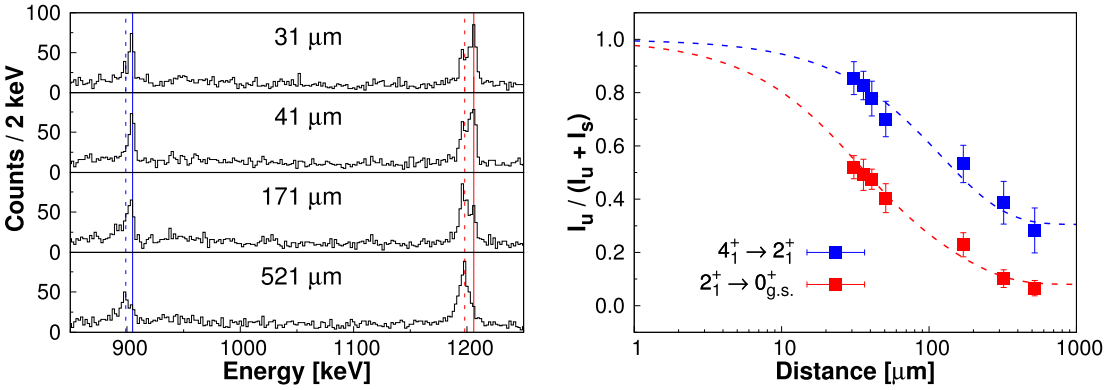

Fig. 2. (left) Doppler-corrected γ-ray energy spectra of ^{108}Sn for different target-to-degrader distances, gated on the Total Kinetic-Energy Loss (TKEL). For each transition the *unshifted* (u) and *shifted* (s) centroids are indicated by a solid and a dashed line, respectively. (right) Ratio of the transition components intensity as a function of the distance, obtained by gating on the TKEL. The dashed lines represent the fitted decay curves for the two excited states.

newly measured $B(E2; 4_1^+ \rightarrow 2_1^+)$ values. Given a proper interaction, it is very simple to describe the "anomalous" $B(E2; 2_1^+ \rightarrow 0^+_{g.s.})$ pattern of the Sn isotopes, while the –hitherto unexplored– $B(E2; 4_1^+ \rightarrow 2_1^+)$ behavior demands more care.

The context of these theoretical results is provided by the Pseudo-SU(3) symmetry, which acts in the space of *gds* orbits above (and except) $g_{9/2}$. The basic idea is inspired by Elliott's SU(3) scheme [31,32] and consists in building intrinsic states that maximize the quadrupole operator [33–35]. As shown in Figure 2 of Ref. [30] (top right pad), for the light Sn nuclei only the first 6 neutrons play a role in the value of the quadrupole operator, while the contribution of the following 6 neutrons is null, leading to a "plateau" in the $B(E2; 2_1^+ \rightarrow 0^+_{g.s.})$ reduced transition probabilities. For a strong enough quadrupole force, the system exhibits rotational features, leading to $B_{4/2} \equiv B(E2; 4_1^+ \rightarrow 2_1^+)/B(E2; 2_1^+ \rightarrow 0^+_{g.s.}) \approx 1.43$ (Alaga rule). This holds in the Cd case, while for Sn the quadrupole strength is much reduced due to the absence of $g_{9/2}$ proton holes. It is still strong enough to produce a stable $B(E2; 2_1^+ \rightarrow 0^+_{g.s.})$ pattern analogous to the Cd one, but the $B(E2; 4_1^+ \rightarrow 2_1^+)$ behavior becomes sensitive to pairing and single-particle behavior. Thus, it appears that the quadrupole dominance in Cd gives way to a form of pairing-quadrupole interplay in Sn. For the sake of completeness, in what follows we briefly explain the steps involved in the shell model calculations.

The interaction must be extracted from a realistic potential, properly renormalized and monopole corrected. All realistic potentials give very similar results [34], N3LO was chosen [46] and V_{low-k}-regularized [47]. The CDB [48] or AV18 [49] potentials would yield the same results. The indispensable renormalizations amount to a –rigorously established– 30% boost of the quadrupole force and a phenomenological 40% increase of the pairing force [50]. The replacement of the monopole term is imperative, since the realistic interactions have bad monopole behavior [34, Sec. II.B.3]. Thus, this correction was done by replacing the monopole part of the interaction with the Hamiltonian provided by the GEMO (GEneral MOnopole) code [51], which is based on the Duflo-Zuker mass formula [52,53], adding the single particle spectrum of ^{101}Sn (in parentheses the energies in MeV):

$$g_{9/2}(-6.0),\ d_{5/2}(0.0),\ g_{7/2}(0.5),\ s_{1/2}(0.8),\ d_{3/2}(1.6).$$

The resulting interaction is called I.3.4. Possible uncertainties concern the pairing content, so the pairing strength has been treated as a free parameter and different values have been investigated, yielding to the I.3.0 and I.3.2 interactions (with no and 20% corrections, respectively). Furthermore, according to the study of Ref. [54, Fig. 3.2.1], an alternative to the GEMO spectrum (DZ in that Figure)

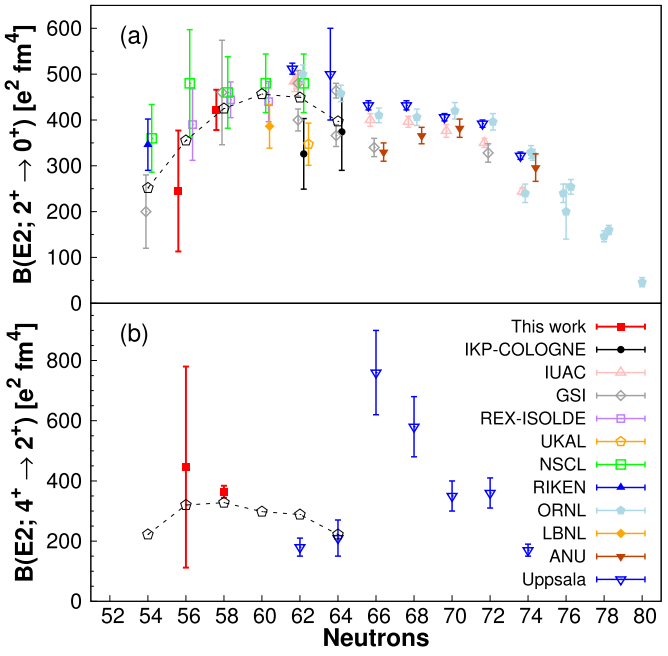

Fig. 3. Reduced transition probability $B(E2)$ for the (a) $2_1^+ \rightarrow 0^+_{g.s.}$ and (b) $4_1^+ \rightarrow 2_1^+$ transitions along the Sn isotopic chain. The results of the present work (red squares) are compared with those from previous experiments [9,36,1–3,37,4,38,5,39–41,6,42,7,43,44,8,45]. The predictions from Large-Scale Shell-Model calculations from the I.3.4 interaction are also shown (open black pentagons).

is an extrapolated estimate (EX) equivalent to pushing up the $s_{1/2}$ orbital to 1.6 MeV, which results in the I.3.4s1.6 interaction.

The calculations were performed with the ANTOINE program [34] in utM spaces in the *gds* shell of up to u $g_{9/2}$-proton holes and t $g_{9/2}$-neutron holes, for a total of M holes. Here we present $utM = 202$ cases of m-scheme dimensions of up to $6 \cdot 10^7$, but it was checked that they reproduce well the 10^{10}-dimensional $utM = 444$ cases.

Fig. 4 (a) establishes that the amount of pairing makes no difference in the $B(E2; 2_1^+ \rightarrow 0^+_{g.s.})$ transition probabilities. The shift in the position of the $s_{1/2}$ orbit has an influence, albeit minor. In the Fig. 4 (b) both the pairing and the single particle shift make an enormous difference in the $B(E2; 4_1^+ \rightarrow 2_1^+)$ behavior. In the case of strong quadrupole dominance, the $B(E2; 2_1^+ \rightarrow 0^+_{g.s.})$ pattern would be as in Fig. 4 (a) and the $B(E2; 4_1^+ \rightarrow 2_1^+)$ one would be the same multiplied by 1.43. This is not far from the 1.25 for the I.3.0 case, as shown in Fig. 4 (c). The $B_{4/2}$ ratio is further reduced for I.3.2, while the proportionality between patterns is completely

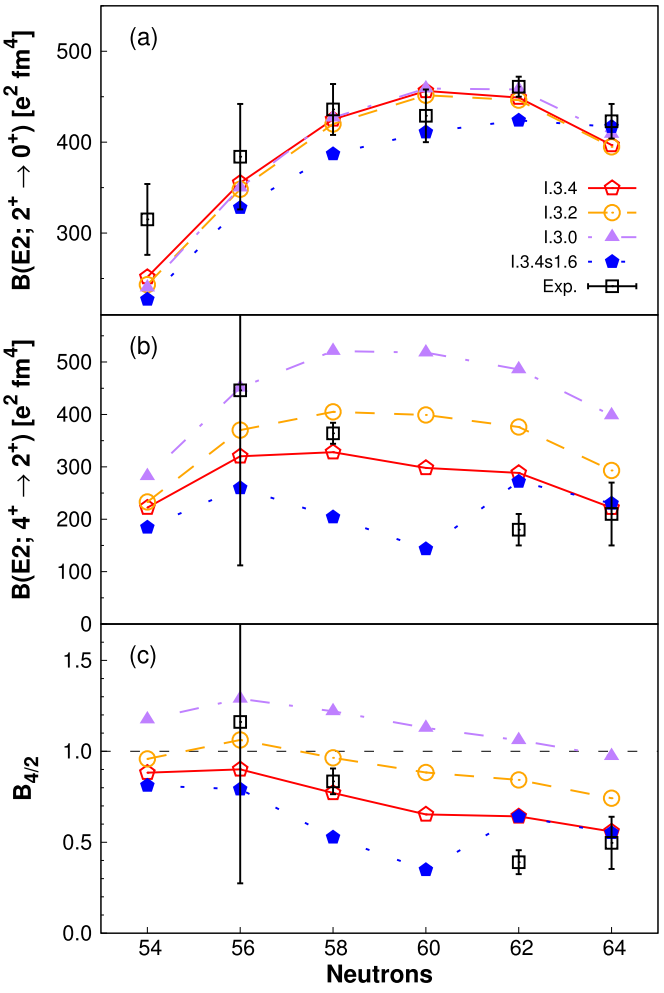

Fig. 4. Experimental and calculated (a) $B(E2;2_1^+ \rightarrow 0_{g.s.}^+)$ and (b) $B(E2;4_1^+ \rightarrow 2_1^+)$ values and (c) $B_{4/2}$ ratio. Effective charges are $(e_\pi, e_\nu) = (1.40, 0.72)$ throughout. For $A = 112$ and 114 the neutron effective charge e_ν should be increased to 0.75 to account for the omission of the $h_{11/2}$ shell, that plays a small but significant role. Experimental $B(E2;2_1^+ \rightarrow 0_{g.s.}^+)$ values are the weighted averages of the Fig. 3 results, while the $B(E2;4_1^+ \rightarrow 2_1^+)$ data comes from Ref. [9] and the present work. I.3.0s1.6 has the $s_{1/2}$ single particle energy moved up by 800 keV with respect to GEMO.

lost for the two I.3.4 cases, but both are close to the observed values in $^{112-114}$Sn [9]. Moreover, our new measure in ^{108}Sn breaks the ambiguity in favor of the I.3.4 chosen standard with GEMO spectrum, providing a potentially interesting suggestion about the spectrum of ^{101}Sn.

Traditionally all emphasis has been put in explaining the $B(E2;2_1^+ \rightarrow 0_{g.s.}^+)$ patterns, while the $B(E2;4_1^+ \rightarrow 2_1^+)$ ones have been ignored. To understand the present situation, we do well to remember that nuclear structure is a compromise between monopole, quadrupole and pairing. Under a favorable monopole structure (and good monopole behavior of the interaction), quadrupole dominance obtains and leads to rotational features. Energies (moments of inertia) are sensitive to pairing, but the $B(E2;2_1^+ \rightarrow 0_{g.s.}^+)$ patterns are immune. This is what seems to be happening in the calculations of Togashi et al. [12], whose $B(E2;2_1^+ \rightarrow 0_{g.s.}^+)$ pattern is identical to ours, while the wave-functions exhibit strong spin and mass dependence in the $g_{9/2}$ proton-hole occupancy, which are nearly constant in our case. We attribute the coincidence in the patterns to good monopole behavior.

In addition to the $B(E2)$ strengths, the theoretical estimations are in good agreement with the excitation energy of the 2_1^+ and 4_1^+ states: besides the I.3.0 that represents the no-pairing limit, the various interactions presented in the paper are within ≈ 200 keV accuracy.

5. Conclusions

The unconventional use of multi-nucleon transfer reactions with a plunger device has allowed us to measure lifetimes in the neutron-deficient ^{106,108}Sn isotopes. Since deep-inelastic reactions directly populate the low-lying excited states of the channels of interest, the experimental limitations caused by the presence of the low-lying isomers were overcome. Moreover, the TKEL-gate technique allowed us to avoid the possible contamination from high-lying states above the 6_1^+ isomers. This led to the first $B(E2;4_1^+ \rightarrow 2_1^+)$ measurement in this mass region. The theoretical results show that the experimental trend of the $B(E2;2_1^+ \rightarrow 0_{g.s.}^+)$ values in the mass region $104 \leq A \leq 114$ can be reproduced within the *gds* model space. Traditionally, pairing was thought to be dominant in the Sn isotopes but the calculations indicate that the rather constant pattern of the $B(E2;2_1^+ \rightarrow 0_{g.s.}^+)$ values is associated to quadrupole dominance, independent of the pairing strength. In the case of $B(E2;4_1^+ \rightarrow 2_1^+)$ values, instead, pairing becomes crucial: it is clear that quadrupole dominance holds for the $J^\pi = 0_{g.s.}^+, 2_1^+$ states, but it is strongly challenged for the 4_1^+ state through mixing with a pairing dominated intruder. On the other hand, the lack of precise information about the 4_1^+ states hinders the characterization of such an intruder state. What is beyond doubt is the importance of the very precise measurements in ^{108}Sn, which have shown to open new perspectives in the understanding of the quadrupole-pairing interplay.

These results represent a step forward to our current knowledge of the region. Indeed, the precise measurement of the $B(E2;4_1^+ \rightarrow 2_1^+)$ value in ^{108}Sn has led to a unique theoretical work which, in addition to discuss in detail the balance between pairing-quadrupole correlations in the nuclear interaction, questions the "goodness" of previous theoretical works. In fact, while many different theoretical works have claimed to reproduce the trend of the reduced transition probabilities $B(E2;2_1^+ \rightarrow 0_{g.s.}^+)$ in the $N = Z = 50$ region, our paper highlights that the $B(E2;2_1^+ \rightarrow 0_{g.s.}^+)$ values are not the only ones to be of key importance for understanding the nuclear structure close to ^{100}Sn; actually, the $B(E2;4_1^+ \rightarrow 2_1^+)$ values, whose theoretical discussion is faced for the very first time in this article, result to be of crucial importance for understanding the nuclear structure of the region.

Further experimental and theoretical studies should focus their attentions on the electromagnetic properties not only of the $2_1^+ \rightarrow 0_{g.s.}^+$ transitions, but also of the $4_1^+ \rightarrow 2_1^+$ ones. This will allow us to shed light on the peculiar structure of the Sn isotopic chain, of the $Z \approx 50$ region and of other regions where similar behavior of the $B(E2)$ strengths have been observed, such as the $N = 50$ isotonic chain. In addition, the proton- and neutron-transfer spectroscopic factors will provide further information on the microscopic nature of the low-lying states in the $Z \approx 50$ region.

Declaration of competing interest

The authors declare that they have no known competing financial interests or personal relationships that could have appeared to influence the work reported in this paper.

Acknowledgement

The authors would like to thank the AGATA and VAMOS collaborations. Special thanks go to the GANIL technical staff for their help in setting up the apparatuses and the good quality beam

and to A. Poves for his fruitful comments. This work was partially supported by the European Union's Seventh Framework Programme for Research and Technological Development (grant no. 262010). A.G. acknowledges the support of the Fondazione Cassa di Risparmio Padova e Rovigo under the project CONPHYT, starting grant in 2017. The work was also supported (B.C, H.L., J.N. and U.J.) by Swedish Research Council under the grant agreements nos. 822-2005-3332, 821-2010-6024, 821-2013-2304, 621-2014-5558 and 2017-0065, and by the Knut and Alice Wallenberg Foundation grant no. 2005.0184, (B.S.) by the Scientific and Technological Council of Turkey (TUBITAK) under the project no. 114F473, (A.G., A.J. and R.P.) by the Ministerio de Ciencia e Innovacíon under the contracts nos. SEV-2014-0398, FPA2017-84756-C4 and EEBB-I-15-09671, by the Generalitat Valenciana under the grant agreement no. PROMETEO/2019/005 and by the EU-FEDER funds, (T.M and S.S.) by the Croatian Science Foundation under the project no. 7194, (I.K and D.S.) by the Hungarian National Research and Innovation Office (NKFIH) under the project nos. K128947, PD124717 and GINOP-2.3.3-15-2016-00034, (M.P.) by the Polish National Science Centre with the grants nos. 2014-14-M-ST2-00738, 2016-22-M-ST2-00269 and 2017-25-B-ST2-01569 under the COPIN-IN2P3, COPIGAL and POLITA projects.

References

[1] A. Banu, J. Gerl, C. Fahlander, M. Górska, H. Grawe, T.R. Saito, H.-J. Wollersheim, E. Caurier, T. Engeland, A. Gniady, M. Hjorth-Jensen, F. Nowacki, T. Beck, F. Becker, P. Bednarczyk, M.A. Bentley, A. Bürger, F. Cristancho, G.d. Angelis, Z. Dombrádi, P. Doornenbal, H. Geissel, J. Grebosz, G. Hammond, M. Hellström, J. Jolie, I. Kojouharov, N. Kurz, R. Lozeva, S. Mandal, N. Mărginean, S. Muralithar, J. Nyberg, J. Pochodzalla, W. Prokopowicz, P. Reiter, D. Rudolph, C. Rusu, N. Saito, H. Schaffner, D. Sohler, H. Weick, C. Wheldon, M. Winkler, ^{108}Sn studied with intermediate-energy Coulomb excitation, Phys. Rev. C 72 (2005) 061305(R).

[2] C. Vaman, C. Andreoiu, D. Bazin, A. Becerril, B.A. Brown, C.M. Campbell, A. Chester, J.M. Cook, D.C. Dinca, A. Gade, D. Galaviz, T. Glasmacher, M. Hjorth-Jensen, M. Horoi, D. Miller, V. Moeller, W.F. Mueller, A. Schiller, K. Starosta, A. Stolz, J.R. Terry, A. Volya, V. Zelevinsky, H. Zwahlen, $Z = 50$ Shell gap near ^{100}Sn from intermediate-energy Coulomb excitations in even-mass $^{106-112}$Sn isotopes, Phys. Rev. Lett. 99 (2007) 162501.

[3] J. Cederkäll, A. Ekström, C. Fahlander, A.M. Hurst, M. Hjorth-Jensen, F. Ames, A. Banu, P.A. Butler, T. Davinson, U.D. Pramanik, J. Eberth, S. Franchoo, G. Georgiev, M. Górska, D. Habs, M. Huyse, O. Ivanov, J. Iwanicki, O. Kester, U. Köster, B.A. Marsh, O. Niedermaier, T. Nilsson, P. Reiter, H. Scheit, D. Schwalm, T. Sieber, G. Sletten, I. Stefanescu, J. Van de Walle, P. Van Duppen, N. Warr, D. Weisshaar, F. Wenander, Sub-barrier Coulomb excitation of ^{110}Sn and its implications for the ^{100}Sn shell closure, Phys. Rev. Lett. 98 (2007) 172501.

[4] A. Ekström, J. Cederkäll, C. Fahlander, M. Hjorth-Jensen, F. Ames, P.A. Butler, T. Davinson, J. Eberth, F. Fincke, A. Görgen, M. Górska, D. Habs, A.M. Hurst, M. Huyse, O. Ivanov, J. Iwanicki, O. Kester, U. Köster, B.A. Marsh, J. Mierzejewski, P. Reiter, H. Scheit, D. Schwalm, S. Siem, G. Sletten, I. Stefanescu, G.M. Tveten, J. Van de Walle, P. Van Duppen, D. Voulot, N. Warr, D. Weisshaar, F. Wenander, M. Zielińska, $0^+_{gs} \to 2^+_1$ transition strengths in ^{106}Sn and ^{108}Sn, Phys. Rev. Lett. 101 (2008) 012502.

[5] R. Kumar, P. Doornenbal, A. Jhingan, R.K. Bhowmik, S. Muralithar, S. Appannababu, R. Garg, J. Gerl, M. Górska, J. Kaur, I. Kojouharov, S. Mandal, S. Mukherjee, D. Siwal, A. Sharma, P.P. Singh, R.P. Singh, H.J. Wollersheim, Enhanced $0^+_{g.s.} \to 2^+_1$ $E2$ transition strength in ^{112}Sn, Phys. Rev. C 81 (2010) 024306.

[6] V.M. Bader, A. Gade, D. Weisshaar, B.A. Brown, T. Baugher, D. Bazin, J.S. Berryman, A. Ekström, M. Hjorth-Jensen, S.R. Stroberg, W.B. Walters, K. Wimmer, R. Winkler, Quadrupole collectivity in neutron-deficient Sn nuclei: ^{104}Sn and the role of proton excitations, Phys. Rev. C 88 (2013) 051301.

[7] P. Doornenbal, S. Takeuchi, N. Aoi, M. Matsushita, A. Obertelli, D. Steppenbeck, H. Wang, L. Audirac, H. Baba, P. Bednarczyk, S. Boissinot, M. Ciemala, A. Corsi, T. Furumoto, T. Isobe, A. Jungclaus, V. Lapoux, J. Lee, K. Matsui, T. Motobayashi, D. Nishimura, S. Ota, E.C. Pollacco, H. Sakurai, C. Santamaria, Y. Shiga, D. Sohler, R. Taniuchi, Intermediate-energy Coulomb excitation of ^{104}Sn: moderate $E2$ strength decrease approaching ^{100}Sn, Phys. Rev. C 90 (2014) 061302.

[8] R. Kumar, M. Saxena, P. Doornenbal, A. Jhingan, et al., No evidence of reduced collectivity in Coulomb-excited Sn isotopes, Phys. Rev. C 96 (2017) 054318.

[9] N. Jonsson, A. Bäcklin, J. Kantele, R. Julin, M. Luontama, A. Passoja, Collective states in even Sn nuclei, Nucl. Phys. A 371 (1981) 333.

[10] A. Ansari, Study of the lowest 2+ excitations and B (E2) transition strengths in relativistic QRPA for Sn-, and Pb-isotopes, Phys. Lett. B 623 (1) (2005) 37.

[11] B. Maheshwari, A. Kumar Jain, B. Singh, Asymmetric behavior of the $B(E2; 0^+ \to 2^+)$ values in $^{104-130}$Sn and generalized seniority, Nucl. Phys. A 952 (2016) 62.

[12] T. Togashi, Y. Tsunoda, T. Otsuka, N. Shimizu, M. Honma, Novel shape evolution in Sn isotopes from magic numbers 50 to 82, Phys. Rev. Lett. 121 (2018) 062501.

[13] S. Szilner, C.A. Ur, L. Corradi, N. Mărginean, G. Pollarolo, A.M. Stefanini, S. Beghini, B.R. Behera, E. Fioretto, A. Gadea, B. Guiot, A. Latina, P. Mason, G. Montagnoli, F. Scarlassara, M. Trotta, G.d. Angelis, F.D. Vedova, E. Farnea, F. Haas, S. Lenzi, S. Lunardi, R. Mărginean, R. Menegazzo, D.R. Napoli, M. Nespolo, I.V. Pokrovsky, F. Recchia, M. Romoli, M.-D. Salsac, N. Soić, J.J. Valiente-Dobón, Multinucleon transfer reactions in closed-shell nuclei, Phys. Rev. C 76 (2007) 024604.

[14] L. Corradi, G. Pollarolo, S. Szilner, Multinucleon transfer processes in heavy-ion reactions, J. Phys. G 36 (2009) 113101.

[15] J.J. Valiente-Dobón, Gamma-ray spectroscopy of neutron-rich nuclei populated via multinucleon-transfer reactions, in: Basic Concepts in Nuclear Physics: Theory, Experiments and Applications, vol. 182, 2016, p. 87.

[16] A. Dewald, S. Harissopulos, P. Von Brentano, The differential plunger and the differential decay curve method for the analysis of recoil distance Doppler-shift data, Z. Phys. A 334 (1989) 163.

[17] A. Dewald, O. Möller, P. Petkov, Developing the recoil distance doppler-shift technique towards a versatile tool for lifetime measurements of excited nuclear states, Prog. Part. Nucl. Phys. 67 (2012) 786.

[18] J.J. Valiente-Dobón, D. Mengoni, A. Gadea, E. Farnea, S.M. Lenzi, S. Lunardi, A. Dewald, T. Pissulla, S. Szilner, R. Broda, F. Recchia, et al., Lifetime measurements of the neutron-rich $N = 30$ isotones ^{50}Ca and ^{51}Sc: orbital dependence of effective charges in the fp shell, Phys. Rev. Lett. 102 (2009) 242502.

[19] S. Pullanhiotan, A. Chatterjee, B. Jacquot, A. Navin, M. Rejmund, Improvement in the reconstruction method for VAMOS spectrometer, Nucl. Instrum. Methods Phys. Res., Sect. B 266 (2008) 4148.

[20] M. Rejmund, B. Lecornu, A. Navin, C. Schmitt, et al., Performance of the improved larger acceptance spectrometer: VAMOS++, Nucl. Instrum. Methods Phys. Res., Sect. A 646 (2011) 184.

[21] M. Vandebrouck, A. Lemasson, M. Rejmund, G. Fremont, J. Pancin, A. Navin, C. Michelagnoli, J. Goupil, C. Spitaels, B. Jacquot, Dual position sensitive MWPC for tracking reaction products at VAMOS++, Nucl. Instrum. Methods Phys. Res., Sect. A 812 (2016) 112.

[22] S. Akkoyun, et al., Agata-advanced gamma tracking array, Nucl. Instrum. Methods Phys. Res., Sect. A 668 (2012) 26.

[23] E. Clément, C. Michelagnoli, G. de France, H.J. Li, A. Lemasson, C.B. Dejean, et al., Conceptual design of the AGATA 1π array at GANIL, Nucl. Instrum. Methods Phys. Res., Sect. A 855 (2017) 1.

[24] B. Bruyneel, B. Birkenbach, J. Eberth, H. Hess, G. Pascovici, P. Reiter, A. Wiens, et al., Correction for hole trapping in AGATA detectors using pulse shape analysis, Eur. Phys. J. A 49 (5) (2013) 1.

[25] A. Lopez-Martens, K. Hauschild, A. Korichi, J. Roccaz, J.P. Thibaud, γ-ray tracking algorithms: a comparison, Nucl. Instrum. Methods Phys. Res., Sect. A 533 (2004) 454.

[26] M. Siciliano, J.J. Valiente-Dobón, A. Goasduff, D. Bazzacco, et al., Study of quadrupole correlations in N=Z=50 region via lifetime measurements, Acta Phys. Pol. B 48 (2017) 331.

[27] M. Siciliano, Study of quadrupole correlations in the neutron-deficient Sn and Cd region via lifetimes measurements, Nuovo Cimento C 40 (2017) 84.

[28] D. Mengoni, J. Valiente-Dobón, E. Farnea, A. Gadea, A. Dewald, A. Latina, Lifetime measurements of neutron-rich nuclei around ^{48}Ca with the CLARA-PRISMA setup, Eur. Phys. J. A 42 (3) (2009) 387.

[29] M. Siciliano, J. Valiente-Dobón, A. Goasduff, Nuclear structure in the neutron-deficient Sn nuclei. TKEL effects on lifetime measurements, EPJ Web Conf. 223 (2019) 01060.

[30] A. Zuker, Quadrupole dominance in light cd and sn isotopes, Phys. Rev. C (2020), accepted for publication.

[31] J.P. Elliott, Collective motion in the nuclear shell model I. Classification schemes for states of mixed configurations, Proc. R. Soc. Lond. (1958) 128.

[32] J.P. Elliott, Collective motion in the nuclear shell model II. The introduction of intrinsic wave-functions, Proc. R. Soc. Lond. (1958) 562.

[33] A.P. Zuker, J. Retamosa, A. Poves, E. Caurier, Spherical shell model description of rotational motion, Phys. Rev. C 52 (1995) R1741.

[34] E. Caurier, G. Martínez-Pinedo, F. Nowacki, A. Poves, A.P. Zuker, The shell model as a unified view of nuclear structure, Rev. Mod. Phys. 77 (2005) 427.

[35] A.P. Zuker, A. Poves, F. Nowacki, S.M. Lenzi, Nilsson-SU3 self-consistency in heavy $N = Z$ nuclei, Phys. Rev. C 92 (2015) 024320.

[36] D.C. Radford, et al., Nuclear structure studies with heavy neutron-rich RIBS at the HRIBF, Nucl. Phys. A 746 (2004) 83.

[37] J.N. Orce, S.N. Choudry, B. Crider, E. Elhami, S. Mukhopadhyay, M. Scheck, M.T. McEllistrem, S.W. Yates, $2^+_1 \to 0^+_1$ transition strengths in Sn nuclei, Phys. Rev. C 76 (2) (2007) 021302(R).

[38] P. Doornenbal, P. Reiter, H. Grawe, H.J. Wollersheim, P. Bednarczyk, L. Caceres, J. Cederkäll, A. Ekström, J. Gerl, M. Górska, A. Jhingan, I. Kojouharov, R. Kumar, W. Prokopowicz, H. Schaffner, R.P. Singh, Enhanced strength of the $2^+_1 \to 0^+_{g.s.}$

transition in ^{114}Sn studied via Coulomb excitation in inverse kinematics, Phys. Rev. C 78 (2008) 031303(R).
[39] J.M. Allmond, D.C. Radford, C. Baktash, J.C. Batchelder, A. Galindo-Uribarri, C.J. Gross, P.A. Hausladen, K. Lagergren, Y. Larochelle, E. Padilla-Rodal, C.-H. Yu, Coulomb excitation of ^{124,126,128}Sn, Phys. Rev. C 84 (2011) 061303(R).
[40] A. Jungclaus, J. Walker, J. Leske, K.H. Speidel, A.E. Stuchbery, M. East, et al., Evidence for reduced collectivity around the neutron mid-shell in the stable even-mass Sn isotopes from new lifetime measurements, Phys. Lett. B 695 (2011) 110.
[41] G. Kumbartzki, et al., Transient field g factor and mean-life measurements with a rare isotope beam of ^{126}sn, Phys. Rev. C 86 (2012) 034319.
[42] G. Guastalla, D.D. Di Julio, M. Górska, J. Cederkäll, P. Boutachkov, P. Golubev, S. Pietri, H. Grawe, F. Nowacki, K. Sieja, et al., Coulomb excitation of ^{104}Sn and the strength of the ^{100}Sn shell closure, Phys. Rev. Lett. 110 (2013) 172501.
[43] J.M. Allmond, A.E. Stuchbery, A. Galindo-Uribarri, E. Padilla-Rodal, D.C. Radford, J.C. Batchelder, C.R. Bingham, M.E. Howard, J.F. Liang, B. Manning, S.D. Pain, N.J. Stone, R.L. Varner, C.-H. Yu, Investigation into the semimagic nature of the tin isotopes through electromagnetic moments, Phys. Rev. C 92 (4) (2015) 041303(R).
[44] G.J. Kumbartzki, N. Benczer-Koller, K.-H. Speidel, D.A. Torres, J.M. Allmond, P. Fallon, I. Abramovic, L.A. Bernstein, J.E. Bevins, H.L. Crawford, Z.E. Guevara, G. Gürdal, A.M. Hurst, L. Kirsch, T.A. Laplace, A. Lo, E.F. Matthews, I. Mayers, L.W. Phair, F. Ramirez, S.J.Q. Robinson, Y.Y. Sharon, A. Wiens, $Z = 50$ core stability in ^{110}Sn from magnetic-moment and lifetime measurements, Phys. Rev. C 93 (2016) 044316.
[45] M. Spieker, P. Petkov, E. Litvinova, C. Müller-Gatermann, S.G. Pickstone, S. Prill, P. Scholz, A. Zilges, Shape coexistence and collective low-spin states in ^{112,114}Sn studied with the $(p, p'\gamma)$ Doppler-shift attenuation coincidence technique, Phys. Rev. C 97 (2018) 054319.
[46] D. Entem, R. Machleidt, Accurate chiral potential, Phys. Lett. B 524 (2002) 93.
[47] S. Bogner, T. Kuo, A. Schwenk, Model-independent low momentum nucleon interaction from phase shift equivalence, Phys. Rep. 386 (1) (2003) 1.
[48] R. Machleidt, F. Sammarruca, Y. Song, Cd bonn, Phys. Rev. C 53 (1996) R1483.
[49] R.B. Wiringa, V.G.J. Stoks, R. Schiavilla, Argonne pots, Phys. Rev. C 51 (1995) 38.
[50] M. Dufour, A.P. Zuker, Realistic collective nuclear Hamiltonian, Phys. Rev. C 54 (1996) 1641.
[51] J. Duflo, A.P. Zuker, GEMO program gemosp9.f in https://www-nds.iaea.org/amdc/, 2000.
[52] J. Duflo, A.P. Zuker, The nuclear monopole Hamiltonian, Phys. Rev. C 59 (1999) R2347.
[53] J. Mendoza-Temis, J.G. Hirsch, A.P. Zuker, The anatomy of the simplest Duflo–Zuker mass formula, Nucl. Phys. A 843 (1) (2010) 14.
[54] T. Faestermann, M. Górska, H. Grawe, The structure of ^{100}Sn and neighbouring nuclei, Prog. Part. Nucl. Phys. 69 (2013) 85.